

# Control of Powders Morphology in the Supercritical Antisolvent Technique Using Solvent Mixtures

Valentina Prosapio, Ernesto Reverchon, Iolanda De Marco\*

University of Salerno, Department of Industrial Engineering, Via Giovanni Paolo II, 84084, Fisciano (SA), Italy  
[idemarco@unisa.it](mailto:idemarco@unisa.it)

The supercritical antisolvent process (SAS) has been frequently used to obtain microparticles and nanoparticles. The fluid dynamics of the process related to the study of the liquid jet in contact with supercritical carbon dioxide (scCO<sub>2</sub>) is characterized by a one-phase mixing at supercritical conditions and a two-phase mixing at subcritical conditions. The transition between the two kinds of mixing can be measured in terms of amplitude of the corresponding pressure range; some organic solvents, like dimethylsulfoxide (DMSO) are characterized by a wide pressure range, other solvents, like acetone (AC), by a narrow pressure range. Generally, microparticles are precipitated by atomization, droplets formation and drying in the transition range, whereas nanoparticles are precipitated in correspondence of completely developed supercritical conditions. Mixing a wide-transition solvent, like DMSO, to a narrow-transition solvent, like acetone, the pressure range of the transition from one-phase mixing to two-phase mixing and, accordingly, the morphology of the precipitates will change.

In this work, two model compounds were SAS processed from DMSO/AC mixtures: cellulose acetate, which is slightly soluble in DMSO and freely soluble in acetone with the aim of obtaining microparticles and polyvinylpyrrolidone (PVP) that is slightly soluble in acetone and freely soluble in DMSO in order to obtain nanoparticles. In the case of cellulose acetate, well-defined microparticles with a mean diameter of 0.42 μm were obtained, whereas, for PVP, nanoparticles with a mean diameter of 114 nm were precipitated, demonstrating that this SAS strategy is successful.

## 1. Introduction

Different supercritical carbon dioxide (scCO<sub>2</sub>) based techniques have been proposed to micronize several kinds of compounds, such as pharmaceuticals, superconductors, coloring matters, explosives, polymers and biopolymers (Shariati and Peters, 2003). In the rapid expansion of supercritical solution (Montes et al., 2013), scCO<sub>2</sub> plays the role of solvent, but, considering that solid materials solubility in scCO<sub>2</sub> is frequently limited, in a great number of scCO<sub>2</sub> based techniques, scCO<sub>2</sub> plays the role of the antisolvent, as in the gas antisolvent precipitation (GAS) (De Marco et al., 2013), in the supercritical antisolvent (SAS) precipitation (Reverchon and De Marco, 2011) or in the expanded liquid antisolvent (ELAS) process (Prosapio et al., 2014). To properly perform SAS process that has been the most used one, scCO<sub>2</sub> has to be completely miscible with the liquid solvent; whereas, the solute has to be insoluble in the mixture solvent/scCO<sub>2</sub>.

To describe the SAS process, the fluid dynamic of the injected solution in contact with scCO<sub>2</sub>, the high-pressure vapor liquid equilibria (VLEs) of the solute/solvent/antisolvent and the mass transfer to and from the injected solution have to be taken into account.

The fluid dynamics of the injected solution in contact with high-pressure carbon dioxide was extensively studied by several authors in SAS literature. For example, Lengsfeld et al. (2000) studied the evolution and disappearance of the liquid surface tension of jets of fluids injected into supercritical carbon dioxide, observing that, at completely miscible conditions, the surface tension vanishes before the jet break-up occurs: a "gas like" jet is then formed. Dukhin et al. (2003) introduced two process characteristic times and their competition; i.e., the jet break-up time and the interfacial tension degradation time. Gokhale et al. (2007) studied the jet atomization in compressed gases, concluding that, at completely developed supercritical conditions, turbulent

one-phase mixing dominates. Those authors also observed that the transition between two-phase (formation of droplets after jet break-up) and one-phase mixing (no formation of droplets) takes place at pressures slightly above the mixture critical pressure (MCP). The non-equilibrium conditions during mixing originate a dynamic (transient) interfacial tension that gradually disappears in the time lag between the inlet of the liquid and its transformation in a gas mixture.

The interaction between the SAS produced morphologies and the high pressure VLEs has been extensively studied. At completely developed supercritical conditions, that is far above the mixture critical point (MCP), nanoparticles are systematically obtained (Torino et al., 2010); at subcritical conditions, i.e. below the MCP of the binary mixture solvent/antisolvent, expanded microparticles were precipitated (Reverchon et al., 2008a); in proximity of the MCP, microparticles are obtained (Reverchon et al., 2008b).

The third main aspect of the process, related to the mass transfer of the three components involved in a SAS experiment, was studied by Werling and Debenedetti in subcritical (1999) and supercritical conditions (2000). Subsequently, Chavez et al. (2003) studied the precipitation process in a droplet, identifying two different mechanisms: a diffusion-limited regime, which produces a precipitation front and a nucleation-limited regime in a homogeneously mixed droplet.

The interactions among the three main aspects of the process on nucleation and growth mechanisms were studied using model compounds (De Marco and Reverchon, 2011a) and modelled (Marra et al., 2012). Using elastic light scattering analysis, Reverchon et al. (2010) proposed a general classification: at subcritical conditions, there is a two-phase mixing, at which expanded microparticles precipitated; at completely developed supercritical conditions, there is a one-phase mixing at which nanoparticles are obtained; the transition region between the two kind of mixing, in which microparticles are produced, takes place in a pressure range whose amplitude varies depending on the solvent used. Subsequently, De Marco et al. (2012) observed that some organic solvent, like dimethylsulfoxide (DMSO) are characterized by a wide pressure range, while other solvents, like acetone (AC) are characterized by a narrow pressure range; moreover, mixtures AC/DMSO show an intermediate behavior between the two solvents and, therefore, it is possible to regulate the amplitude of the transition region and change the morphology of the precipitates.

The aim of this work is to verify these experimental evidences using a solute. For this purpose, two model compounds were SAS processed using mixtures AC/DMSO as solvent: cellulose acetate, which is poorly soluble in DMSO and freely soluble in AC with the aim of obtaining microparticles and polyvinylpyrrolidone (PVP), which is poorly soluble in AC and freely soluble in DMSO in order to obtain nanoparticles.

## 2. Experimental section

### 2.1 Materials

Cellulose acetate (CA, degree of substitution = 2.5,  $M_w \approx 50,000$ ), Polyvinylpyrrolidone (PVP,  $M_w = 10$  kg/mol), acetone (AC, purity 99.8%), and dimethylsulfoxide (DMSO, purity 99.5%) were supplied by Sigma–Aldrich (Italy).  $CO_2$  (purity 99%) was purchased from S.O.N. (Società Ossigeno Napoli, Italy). All materials were used as received.

### 2.2 Apparatus, procedures and analyses

A scheme of the SAS apparatus is reported in Figure 1.

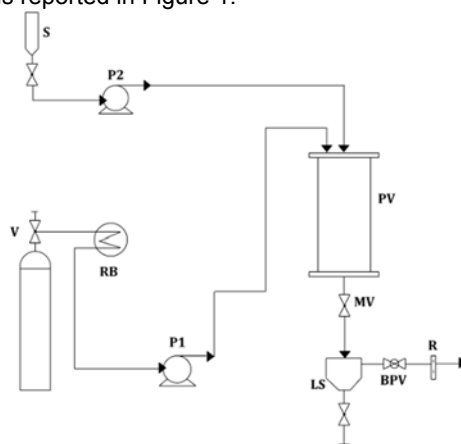


Figure 1: Schematic representation of SAS apparatus. V:  $CO_2$  supply; S: liquid solution; RB: refrigerating bath; P1, P2: pumps; PV: precipitation vessel; MV: micrometering valve; LS: liquid separator; BPV: back-pressure valve; R: rotameter.

The plant mainly consists of two pumps used to deliver the liquid solution and supercritical CO<sub>2</sub>, respectively. A cylindrical vessel of 500 cm<sup>3</sup> internal volume (I.V.) (i.d. = 5 cm) is used as precipitation chamber. The liquid mixture is delivered to the precipitator through a stainless steel nozzle. Carbon dioxide is cooled in a refrigerating bath, before pumping, to avoid cavitation, and, after a preheating, is co-current delivered through another port to the chamber. The temperature is assured by a PID controller connected with electrically thin banders and the pressure in the chamber is measured using a test gauge manometer and regulated by a micrometering valve. A stainless steel frit (pore diameter of 0.1 μm) located at the bottom of the chamber is used to collect the produced powder. A second vessel located downstream the micrometering valve, which pressure is regulated by a backpressure valve, is used to recover the liquid solvent. At the exit of the second vessel, the CO<sub>2</sub> flow rate is measured by a rotameter. A SAS experiment usually begins delivering CO<sub>2</sub> to the SAS vessel until the desired pressure is reached. When antisolvent steady flow is established, the mixture of organic solvents is sent through the nozzle to the chamber for at least 15 min. When a quasi-steady state composition of solvents and antisolvent is realized inside the SAS vessel, the flow of the solvents is stopped and the liquid solution is delivered through the nozzle, producing the precipitation of the solute. At the end of the solution delivery, supercritical CO<sub>2</sub> continues to flow, to wash the chamber, eliminating the solution formed by the liquid solubilized in the supercritical antisolvent. At the end of the washing step, CO<sub>2</sub> flow is stopped and the precipitator is depressurized down to atmospheric pressure.

Samples of the precipitated powder were collected at different points inside the precipitation chamber and examined using a Field Emission Scanning Electron Microscope (FESEM, mod. LEO 1525, Carl Zeiss SMT AG, Oberkochen, Germany). FESEM samples were covered with 250 Å of gold using a sputter coater (Agar, mod. 108A). Particle size (PS) and particle size distribution (PSD) were measured using an image processing software (Sigma Scan Pro, Jandel Scientific) that counts, measures, and analyzes digital images. About 1000 particles, coming from different images, were considered for each PSD calculation.

### 3. Results and discussion

#### 3.1 Microparticles production

When a compound is soluble only in solvents characterized by a narrow transition between two phase and one phase mixing, it is very difficult to obtain microparticles since, passing from subcritical to supercritical conditions, nanoparticles are immediately produced. CA is a polymer which shows a low solubility in DMSO (and in other solvents with a broad transition region) and, until now, when SAS processed using acetone, never produced microparticles (De Marco and Reverchon, 2011b). To verify if the use of solvent mixtures can overcome this limitation, some precipitation experiments were made using mixtures AC/DMSO in different percentages of the two solvents.

The experiments were carried out at 85 bar, 40 °C, 40 mg of CA for mL of liquid solvent and a nozzle diameter of 100 μm. The liquid solution flow rate was fixed at 1 mL/min and the CO<sub>2</sub> molar fraction was equal to 0.98. In Table 1, a list of the experiments performed with the solvent used, the morphology obtained, the mean diameter (m.d.) and the standard deviation (s.d.) is reported.

Table 1: SAS experiments performed on Cellulose Acetate. NP: nanoparticles; MP: microparticles.

Solvent	Morphology	m.d. (μm)	s.d. (μm)
AC	NP	0.097	0.020
AC/DMSO 75/25	MP	0.403	0.160
AC/DMSO 50/50	MP	0.424	0.155
AC/DMSO 25/75	Coalescing MP	-	-

As observed in Figure 2a, nanoparticles with a narrow size distribution were precipitated when pure acetone was used as solvent, confirming literature results. The use of the mixtures AC/DMSO 75/25 and AC/DMSO 50/50 led, instead, the production of well-defined microparticles, as reported in Figure 2b and 2c. When the mixture AC/DMSO 25/75 was used, the produced particles were coalescing and cannot be characterized in terms of dimensions (Figure 2d). In Figure 3, a comparison between the volumetric particle size distributions of particles obtained using the different mixtures is reported. Increasing the amount of DMSO in the processed solution, the mean diameter of the precipitated particles increased and the particle size distribution enlarged.

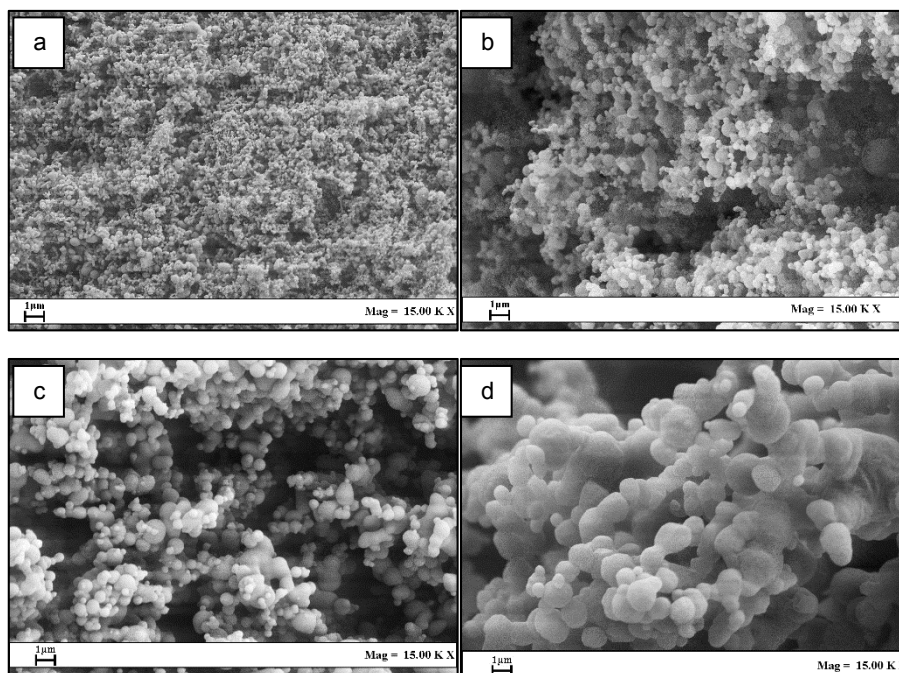


Figure 2: FESEM images of CA particles precipitated at different AC/DMSO mixtures percentages: (a) pure AC; (b) 75/25 (v/v); (c) 50/50 (v/v); (d) 25/75 (v/v).

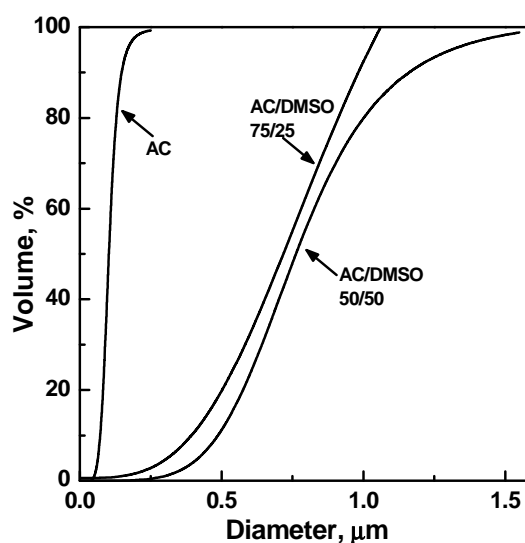


Figure 3: Volumetric cumulative particle size distribution of the CA particles precipitated at different AC/DMSO mixtures percentages.

### 3.2 Nanoparticles production

In some cases, it can be important to produce nanoparticles at ordinary SAS operating conditions. For compounds that are soluble only in solvents with a broad pressure transition interval from two-phase to one-phase mixing, it can be difficult to obtain nanoparticles, even working at high pressure values. For example, polyvinylpyrrolidone (PVP), a polymer soluble in DMSO and in other solvents with a broad transition region from two-phase to one-phase mixing, which, when processed with SAS technique, precipitated always in form of microparticles. In order to produce PVP nanoparticles, some precipitation experiments were performed using AC/DMSO mixtures in different proportions of the two solvents.

The experiments were carried out at 150 bar, 40 °C, 20 mg of PVP for mL of liquid solvent and a nozzle diameter of 100 μm. The liquid solution flow rate was fixed at 1 mL/min and the CO<sub>2</sub> molar fraction was equal to 0.98. A list of the experiments performed with the solvent used, the morphology obtained, the mean diameter (m.d.) and the standard deviation (s.d.) is reported in Table 2.

Table 2: SAS experiments performed on PVP. NP: nanoparticles; MP: microparticles.

Solvent	Morphology	m.d. ( $\mu\text{m}$ )	s.d. ( $\mu\text{m}$ )
DMSO	MP	3.801	2.406
AC/DMSO 25/75	NP	0.313	0.041
AC/DMSO 50/50	NP	0.252	0.065
AC/DMSO 75/25	NP	0.114	0.038

When pure DMSO was used, PVP precipitated in form of spherical microparticles with a mean diameter of 3.8  $\mu\text{m}$ , as it is possible to observe from Figure 4a. Using the mixture AC/DMSO, instead, nanoparticles were produced, as reported in Figures 4b-4d. A comparison among the volumetric particle size distributions of particles obtained using the different mixtures is reported in Figure 5.

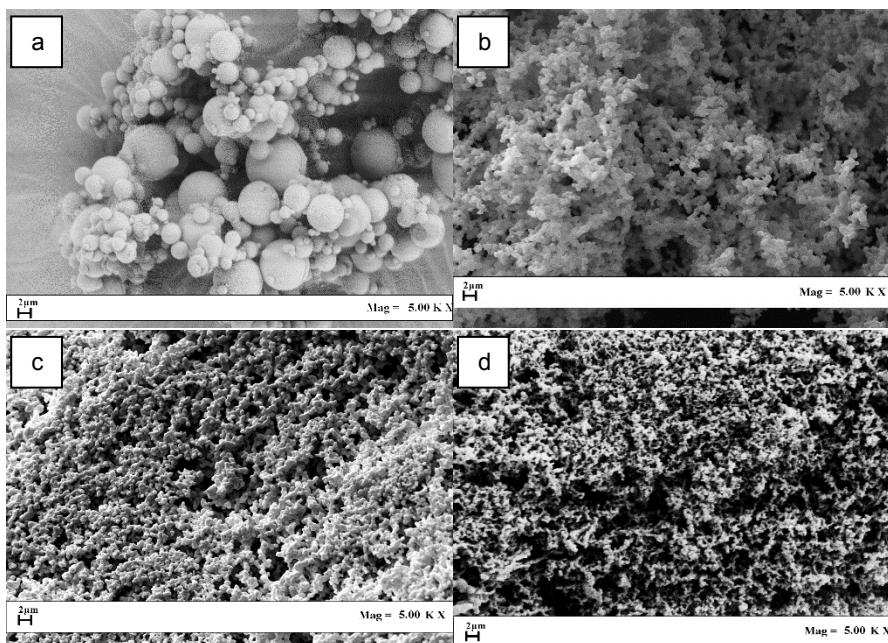


Figure 4: FESEM images of PVP particles precipitated at different AC/DMSO mixtures percentages: (a) 0/100; (b) 25/75 (v/v); (c) 50/50 (v/v); (d) 75/25 (v/v).

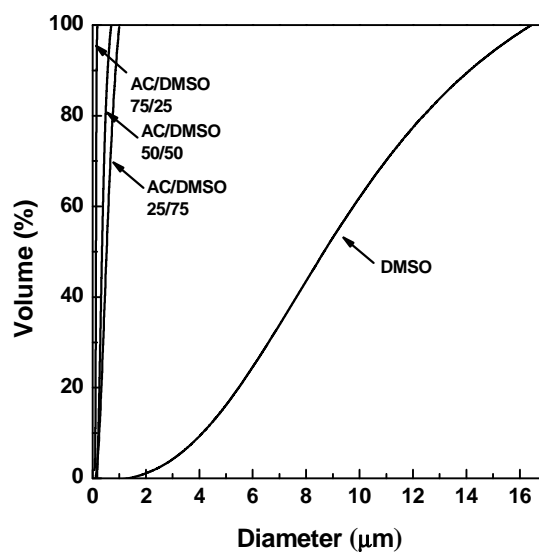


Figure 5 Volumetric cumulative particle size distributions of the PVP particles precipitated at different AC/DMSO mixtures percentages.

Looking at Figure 5, it is possible to note that adding AC to DMSO, the dimension of the particles shrank dramatically; in particular, increasing the quantity of AC in the liquid solution, the mean size reduced and the PSD become narrower.

#### 4. Conclusions

The results obtained in these experiments confirmed that solvent mixtures, formed by a sharp two-phase/one-phase mixing transition solvent (like AC) plus a broad two-phase/one-phase mixing transition solvent (like DMSO), not only show intermediate behaviors between the two solvents during SAS processing, but allow to change the morphology of the precipitates. Indeed:

- In the case of cellulose acetate, the use of AC/DMSO mixtures led the production of microparticles, which had never been obtained before;
- In the case of PVP, the use of solvent mixtures has proved to be effective in the production of nanoparticles, never obtained till date using pure solvents.

#### References

- Chavez F., Debenedetti P.G., Luo J.J., Dave R.N., Pfeffer R., 2003, Estimation of the characteristic time scales in the supercritical antisolvent process, *Ind. Eng. Chem. Res.* 42(13), 3156–3162.
- De Marco I., Reverchon E., 2011a, Influence of pressure, temperature and concentration on the mechanisms of particle precipitation in supercritical antisolvent micronization, *J. Supercritical Fluids* 58, 295–302.
- De Marco I., Reverchon E., 2011b, Nanostructured cellulose acetate filaments produced by supercritical antisolvent precipitation, *J. Supercritical Fluids* 55, 1095–1103.
- De Marco I., Knauer O., Cice F., Braeuer A., Reverchon E., 2012, Interactions of phase equilibria, jet fluid dynamics and mass transfer during supercritical antisolvent micronization: The influence of solvents, *Chem. Eng. J.* 203, 71–80.
- De Marco I., Cardea S., Reverchon E., 2013, Polymer Micronization using Batch Supercritical Antisolvent Process, *Chemical Engineering Transactions* 32, 2185–2190.
- Dukhin S. S., Zhu C., Dave R., Pfeffer R., Luo J.J., Chavez F., Shen Y., 2003, Dynamic interfacial tension near critical point of a solvent–antisolvent mixture and laminar jet stabilization, *Colloids and Surfaces A: Physicochemical and Engineering Aspects* 229 (1–3), 181–199.
- Gokhale A., Khusid B., Dave R.N., Pfeffer R., 2007, Effect of solvent strength and operating pressure on the formation of submicrometer polymer particles in supercritical microjets, *J. Supercritical Fluids* 43 (2), 341–356.
- Lengsfeld C. S., Delplanque J. P., Barocas V. H., Randolph T.W., 2000, Mechanism governing microparticle morphology during precipitation by a compressed antisolvent: atomization vs. nucleation and growth, *J. Physical Chemistry B* 104, 2725–2735.
- Marra F., De Marco I., Reverchon E., 2012, Numerical analysis of the characteristic times controlling supercritical antisolvent micronization, *Chem. Eng. Sci.* 71, 39–45.
- Montes A., Gordillo M.D., Pereyra C.M., Di Giacomo G., Martínez de la Ossa E.J., 2013, Poli (L-lactide) Micronization by Supercritical Fluids, *Chemical Engineering Transactions* 32, 2215–2220.
- Prosapio V., Reverchon E., De Marco I., 2014, Antisolvent micronization of BSA using supercritical mixtures carbon dioxide + organic solvent, *J. Supercritical Fluids* 94, 189–197.
- Reverchon E., De Marco I., Adami R., Caputo G., 2008a, Expanded micro-particles by supercritical antisolvent precipitation: interpretation of results, *J. Supercritical Fluids* 44, 98–108.
- Reverchon E., Adami R., Caputo G., De Marco I., 2008b, Spherical microparticles production by supercritical antisolvent precipitation: interpretation of results, *J. Supercritical Fluids* 47, 70–84.
- Reverchon E., Torino E., Dowy S., Braeuer A., Leipertz A., 2010, Interactions of phase equilibria, jet fluid dynamics and mass transfer during supercritical antisolvent micronization, *Chem. Eng. J.* 156, 446–458.
- Reverchon E., De Marco I., 2011, Mechanisms controlling supercritical antisolvent precipitate morphology, *Chem. Eng. J.* 169, 358–370.
- Shariati A., Peters C.J., 2003, Recent developments in particle design using supercritical fluids, *Curr. Opin. Solid State & Mater. Sci.* 7 (4–5), 371–383.
- Torino E., De Marco I., Reverchon E., 2010, Organic nanoparticles recovery in supercritical antisolvent precipitation, *J. Supercritical Fluids* 55, 300–306.
- Werling J.O., Debenedetti P.G., 1999, Numerical modelling of mass transfer in the supercritical antisolvent process, *J. Supercritical Fluids* 16(2), 167–181.
- Werling J.O., Debenedetti P.G., 2000, Numerical modelling of mass transfer in the supercritical antisolvent process: miscible conditions, *J. Supercritical Fluids* 18(1), 11–24.